Published in final edited form as:
Biomaterials. 2012 January ; 33(2): 524–534. doi:10.1016/j.biomaterials.2011.09.080.

Increasing the pore sizes of bone-mimetic electrospun scaffolds comprised of polycaprolactone, collagen I and hydroxyapatite to enhance cell infiltration

Matthew C. Phipps[a], **William C. Clem**[b], **Jessica M. Grunda**[c], **Gregory A. Clines**[c], and **Susan L. Bellis**[a,b,*]

[a]University of Alabama at Birmingham, Department of Physiology and Biophysics, United States

[b]University of Alabama at Birmingham, Department of Biomedical Engineering, United States

[c]University of Alabama at Birmingham, Department of Medicine, Division of Endocrinology, Diabetes and Metabolism, United States

Abstract

Bone-mimetic electrospun scaffolds consisting of polycaprolactone (PCL), collagen I and nanoparticulate hydroxyapatite (HA) have previously been shown to support the adhesion, integrin-related signaling and proliferation of mesenchymal stem cells (MSCs), suggesting these matrices serve as promising degradable substrates for osteoregeneration. However, the small pore sizes in electrospun scaffolds hinder cell infiltration in vitro and tissue-ingrowth into the scaffold in vivo, limiting their clinical potential. In this study, three separate techniques were evaluated for their capability to increase the pore size of the PCL/col I/nanoHA scaffolds: limited protease digestion, decreasing the fiber packing density during electro-spinning, and inclusion of sacrificial fibers of the water-soluble polymer PEO. The PEO sacrificial fiber approach was found to be the most effective in increasing scaffold pore size. Furthermore, the use of sacrificial fibers promoted increased MSC infiltration into the scaffolds, as well as greater infiltration of endogenous cells within bone upon placement of scaffolds within calvarial organ cultures. These collective findings support the use of sacrificial PEO fibers as a means to increase the porosity of complex, bone-mimicking electrospun scaffolds, thereby enhancing tissue regenerative processes that depend upon cell infiltration, such as vascularization and replacement of the scaffold with native bone tissue.

Keywords

Bone tissue engineering; Cellular infiltration; Porosity; Scaffold; Biomimetic material; Organ culture

1. Introduction

Although significant advances have been made in the development of biomaterials for bone repair, there is still a pressing need for viable clinical alternatives to bone autografting [1], which is currently the gold standard treatment [2]. Autografting presents multiple drawbacks for the patient, including increased surgery time, donor site pain, and limited quantity of harvestable bone [2-5]. Biomaterials capable of promoting osteoregeneration would provide

*Corresponding author. University of Alabama at Birmingham, Department of Physiology and Biophysics, Birmingham, AL 35294, United States. Tel.: +1 205 934 3441; fax: +1 205 975 9028. bellis@uab.edu (S.L. Bellis).

a promising solution for many common clinical procedures, such as repair of long bone defects, spinal fusions, craniofacial and dental surgeries [6]. Some of the fundamental features of biomaterials thought to be important for effective bone regeneration include: (i) a biochemical composition and structure that supports osteogenic cell responses, (ii) appropriate kinetics of biodegradability, without any release of toxic byproducts, and (iii) a highly interconnected porous network that allows for proper tissue ingrowth and vascularization of the biomaterial [7].

In order to engineer a successful osteoinductive material, many researchers have turned toward the process of electrospinning [8-12]. Electrospinning has garnered substantial attention in recent years due to the relatively simple fabrication process, combined with the significant potential to tailor these materials to mimic native bone matrices. Electrospun scaffolds have a nanofibrous structure with interconnecting pores and a large surface to volume ratio, resembling natural extracellular matrix (ECM), and are also amenable to the incorporation of biological factors that influence cellular fate [11,13]. Several investigators have developed electrospun scaffolds that combine degradable polymers such as polycaprolactone (PCL) with native bone matrix molecules including collagen I and hydroxyapatite (HA) [13-18]. For example, we previously reported that scaffolds composed of blended PCL/collagen I nanofibers, with nanoparticles of HA distributed throughout the thickness of the matrix, promoted greater mesenchymal stem cell (MSC) adhesion, cell spreading, activation of focal adhesion kinase, and cell proliferation, as compared with scaffolds composed of PCL alone [19]. Thus, the PCL/col/HA scaffolds represent promising substrates for supporting endogenous cells in bone-healing environment, and also have potential utility as a delivery vehicle for exogenously expanded MSCs.

However, one known limitation of electrospun scaffolds is that the pore sizes within the matrices are typically too small to allow efficient cellular infiltration [20-24]. Migration of cells into a biodegradable scaffold is a crucial step for the success of the synthetic graft and the overall healing of the bone defect [20]. Additionally, the small pore sizes constrain vascularization of the biomaterial, which restricts nutrient delivery and waste removal, limiting the amount of tissue-ingrowth that can be supported [20]. To overcome this problem, numerous investigators have proposed mechanisms for increasing the average pore size of electrospun scaffolds with varying levels of success. Pham et al. addressed this issue by alternating layers of microfibers with nanofibers, however cell infiltration under static culture conditions was minimal [25]. Also, the decrease in the number of nanofibers resulting from this method caused diminished cell spreading. Others have used common engineering techniques of salt leaching [26,27] or cryogenic electrospinning [28] and have achieved moderate success, however these techniques require advanced electrospinning setups and can also affect the surface properties of the nanofibers. Another potentially useful approach involves reducing the packing density of the electrospun scaffolds during the fabrication process [29], or alternatively, decreasing the packing density post-electrospinning by employing an ultrasonication method to mechanically separate the fibers, resulting in greater pore sizes and enhanced cellular infiltration [30]. Lastly, several investigators have explored co-electrospinning sacrificial fibers along with stable fibers, thereby creating larger pores after removal of the sacrificial fibers; this strategy has been successful in facilitating cell infiltration [24,31,32].

Despite the many new electrospinning techniques developed to increase scaffold pore size, the vast majority of studies in this area have focused on scaffolds composed solely of synthetic polymers, which offer minimal biologic cues for cells. Therefore it is essential for these techniques to be adapted in order to engineer custom, complex matrices that incorporate biological molecules specific for their intended application. In this study, our

goal was to compare various methods for increasing the pore size of bone-mimetic, PCL/col/HA ("TRI") electrospun scaffolds in order to facilitate the infiltration of osteogenic cells.

2. Materials and methods

2.1. Preparation of electrospun scaffolds

TRI component and PCL electrospun scaffolds were fabricated as described previously [19]. Briefly, electrospinning solutions of 50wt% PCL + 30wt% collagen I + 20wt% HA (TRI), and 100wt% PCL were dissolved in hexafluoroisopropanol (HFP, Sigma–Aldrich) so that the solid weight was 7.5% of the total solution weight. PEO was dissolved in HFP so that the solid weight was 5.5% of the total solution weight. PCL (MW = 100,000 Da) was purchased from Scientific Polymer Products (Ontario, NY), PEO (MW = 200,000 Da) was purchased from Polysciences, Inc. (Warrington, PA), lyophilized calf skin collagen I was from MP Biomedicals (Solon, OH), and HA nanoparticles (20–50 nm) were purchased from Berkeley Advanced Biomaterials, Inc. (San Leandro, CA). The solutions were magnetically stirred at room temperature for over 1 h followed by brief sonication before loading into disposable 3 cc syringes. A voltage of 22.5 kV was applied using a high-voltage power supply (Gamma High Voltage Research, Ormond Beach, FL). The grounded aluminum collection plate (9 cm diameter) was located 15 cm from the tip of the electrically charged 27-gauge needle (Jensen Global Inc., Santa Barbara, CA). A syringe pump (Harvard Apparatus) was used to feed polymer solution into the needle at a flow rate of 2 ml/h. The resulting samples were randomly arranged fibers deposited as a sheet with average thickness of 300 μm. A Humboldt Boring Machine (Fisher) was then used to cut out electrospun scaffolds in fixed diameter circles to insure equal sample size. No chemical or radiation-induced cross-linking of PCL, PEO or collagen fibers was performed.

For studies aimed at reducing the packing density of electrospun scaffolds, a unique collecting plate was used. As shown in Fig. 4A, a plastic petri dish (9 cm diameter) was added to cover the grounded aluminum collecting plate. Twenty evenly spaced 19 gauge (1.5" length) needles (Jensen Global) were inserted perpendicularly through holes created in the petri dish, touching the aluminum plate underneath.

Following electrospinning, samples were placed under vacuum for 48 h to remove the residual HFP solvent. Scaffolds were sterilized in 70% EtOH for 1 h prior to use.

2.2. Implantation of scaffolds into rat tibiae

PCL or TRI scaffolds were implanted into cortical defects created in rat tibias of four male Sprague–Dawley rats as previously described [33] (two rats per scaffold type). The wounds were closed with vicryl sutures, and buprenorphine was given as an analgesic. The tibiae, with implants in place, were retrieved after 7 days, fixed in 4% formalin, and embedded in poly(methylmethacrylate). Multiple 5 μm sections were stained with Goldner's Trichrome, which stains mineralized tissue green, non-mineralized extracellular matrix red, and cell nuclei black. Low power survey images were acquired with a Nikon SMZ-U stereomicroscope. Higher magnification bright field images were acquired with a Nikon Eclipse TE2000-U. NIH guidelines for the care and use of laboratory animals (NIH publication #85-23 rev.1985) were observed, and all protocols were performed with prior approval from the University of Alabama Institutional Animal Care and Use Committee.

2.3. Scanning electron microscopy (SEM) imaging of electrospun scaffolds

Electrospun scaffolds were visualized for fiber integrity and architecture using scanning electron microscopy. For collagenase treatment testing, scaffolds were placed in a collagenase solution (2 mg/ml Roche Applied Sciences) for one week prior to being dried in

increasing gradients of ethanol in water. SEM imaging was performed on a Philips 515 SEM with an accelerating voltage of 15 kV.

In the subcutaneous skin pouch studies, scaffolds were implanted into dorsal subcutaneous sites of male Sprague–Dawley rats as described previously [34]. After one week, animals were sacrificed and implants were retrieved and washed. Scaffolds were dried in gradients of ethanol in water followed by a gradient of hexamethyldisilazane in ethanol. SEM imaging was performed on a Philips 515 SEM with an accelerating voltage of 15 kV.

For reduced packing density studies, SEM imaging was performed on a Philips XL-30 SEM with an accelerating voltage of 10 kV. Scaffolds were dried in a desiccator for 48 h prior to imaging.

2.4. Isolation and culture of MSCs

For *in vitro* infiltration studies, human MSCs were isolated from bone marrow donations, as previously described [35]. Briefly, cells were pelleted by centrifugation, resuspended in Dulbecco's Modified Eagle Medium (DMEM), and then applied to a Histopaque-1077 column (Sigma, St. Louis, MO). A density gradient was generated by centrifugation at 500 *g* for 30 min. Cells from the DMEM/Histopaque interface were extracted with a syringe and seeded onto tissue culture dishes and cultured in DMEM containing 10% fetal bovine serum. Bone marrow samples were obtained with approval from the University of Alabama Institutional Review Board. For fluorescent studies, lentivirus-transduced human MSCs containing green fluorescent protein (GFP) were provided by the Tulane Center for Gene Therapy (New Orleans, LA).

2.5. Collagenase treatment of electrospun scaffolds

TRI scaffolds were treated with a 2 mg/ml collagenase solution at 37 °C for one week. The dry weight of the scaffolds was measured before collagenase treatment, and then the scaffolds were dried in a desiccator before being weighed again. The change in mass is presented as the percent change between the initial and final weighing. 100% PCL scaffolds were used as control.

2.6. MSC infiltration into electrospun scaffolds

MSC infiltration into electrospun scaffolds was tested in two separate experiments. In the first, TRI or PCL scaffolds were treated with collagenase solution (2 mg/ml) overnight prior to being sterilized in 70% ethanol for 1 h. Scaffolds were placed in 24-well CellCrowns™ (Scaffdex, Tampere, Finland) to maintain scaffold orientation. GFP-expressing MSCs were seeded at a density of 3.8×10^4 cells/cm^2 onto the top of the scaffolds and cultured ingrowth media (DMEM containing 4.5 g/L glucose, supplemented with 10% fetal bovine serum) at 37 °C, exchanging media every 2–3 days. After two weeks, cells on the scaffolds were fixed in 70% EtOH prior to embedding the cell-loaded scaffolds in frozen HistoPrep blocks (Fisher Scientific). 6 μm sections were cut using a Leica cryostat. Sections were visualized using a Nikon fluorescent microscope for presence of GFP-expressing cells within the scaffold.

In the second cell infiltration assay, TRI/PEO or TRI scaffolds were washed overnight to remove PEO fibers prior to being sterilized in 70% ethanol for 1 h. Scaffolds were again placed in 24-well CellCrown™ and MSCs were seeded at a density of 5×10^4 cells/cm^2 onto the top of the scaffolds and cultured ingrowth media for one week. Cells were then fixed in 70% EtOH prior to embedding the cell-loaded scaffolds in frozen HistoPrep blocks. 6 μm sections were cut using a Leica cryostat. Sections were stained with DAPI to visualize the location of cell nuclei.

2.7. Removal of sacrificial fibers of PEO

After electrospinning, sacrificial fibers of PEO were removed from electrospun scaffolds by soaking in H_2O overnight at room temperature. The removal of PEO fibers was visualized by adding fluorescent dyes to the electrospinning solutions prior to electrospinning. The green fluorescent dye $DiOC_{18}(3)$ (Invitrogen Corp., Carlsbad, CA) was added to TRI solutions, and the red fluorescent dye $DiIC_{18}(3)$ (Invitrogen) was added to PEO solutions.

For percent mass loss studies, scaffolds were weighed before soaking in water for one week, then dried in a desiccator before being weighed again. The change in mass is presented as the percent change between the initial and final weighing.

2.8. Measuring pore sizes of TRI/PEO scaffolds

TRI/PEO and TRI solutions were electrospun onto glass coverslips attached to the collecting plate. 0.05 mL of solution was electrospun for all samples to ensure equal scaffold thickness. TRI solutions were fluorescently stained with $DiOC_{18}(3)$. After washing scaffolds, the fibers were visualized fluorescently using a Zeiss LSM 710 Confocal microscope. 10um sections were captured by stacking consecutive image slices. Images were analyzed using the Area Auto Detect feature on the NIS-Elements Basic Research software (Nikon Instruments Inc., Melville, NY). The macro was used to automatically detect boundaries and measure areas between fluorescent fibers of 25 pores manually selected at random for each image. Three images were analyzed per sample, two samples per group. All images were taken at 20*x*. Average pore size was calculated using the imaging software.

2.9. Infiltration of cells from calvarial organ cultures

4-day-old Swiss White mice pups were euthanized via decapitation. The calvarial bones were excised as described by Mohammad et al. [36] and placed on top of a steel grid in 6-well plates. Electrospun scaffolds of TRI or TRI/PEO (soaked in water overnight to remove PEO) were placed on top of the calvaria. Calvaria were cultured in serum free media for eight days. Calvaria/scaffold constructs were then fixed in 70% EtOH and embedded in frozen HistoPrep blocks. 6 μm sections were cut using a Leica cryostat. Sections were stained with DAPI to visualize the location of endogenous cell nuclei.

2.10. Statistics

Percent mass loss studies were performed at least two independent times. MSC infiltration studies were performed two independent times in triplicate. Two representative microscopic fields were analyzed per sample, giving a total of 12 fields analyzed for each scaffold formulation. Organ culture studies were performed with seven samples per group. Two representative fields were analyzed per sample, giving a total of 14 fields analyzed for each scaffold type. Data sets were assessed using an unpaired Student's *t*-test parametric analysis, and data were reported as mean + standard deviation. A confidence level of at least 95% ($p < .05$) was considered significant and denoted by "*". Additionally, ($p < .0001$) was denoted by "**".

3. Results

3.1. Controlled degradation of collagen fibers

Previous studies have shown that bone-mimetic electrospun scaffolds consisting of PCL, collagen I and nanoHA ("TRI") support MSC responses *in vitro* that are favorable for new bone formation [19]. However, it has become apparent that the small pore sizes within these scaffolds restrict cellular infiltration, consistent with most other types of electrospun scaffolds. As can be seen in Fig. 1A, TRI scaffolds implanted into a cortical defect created

in a rat tibia supported excellent new bone formation, and higher magnification images (Fig. 1B) revealed that newly synthesized bone was in direct contact with the implant surface. However cells lined the surface of TRI scaffolds, with minimal infiltration into the scaffold (inset in Fig. 1B).

To address this issue, we first tested whether the collagen present in the TRI scaffolds could be used to our advantage as a target for controlled degradation, thereby creating larger pores in order to facilitate cellular infiltration. We hypothesized that a limited treatment with collagenase solution could be employed to introduce selective fiber breaks (without completely eliminating collagen from the scaffolds). To test this, TRI scaffolds, and PCL scaffolds as a control, were treated with collagenase, and substrates were then analyzed by SEM to screen for the presence of fiber breakages. As shown in Fig. 2A, SEM images of the treated scaffolds revealed breakage of fibers in the TRI (e) but not PCL (b) scaffolds. This cleavage of fibers in TRI scaffolds was also observed when scaffolds were placed into rat subcutaneous skin pouches, where they are exposed to endogenous collagenases (f). Additionally, the cleavage of collagen fibers was confirmed by comparing the dry weight of scaffolds before and after treatment with collagenase solution *in vitro*. On average, TRI scaffolds lost 15.6% of their mass after one week, while PCL scaffolds exhibited no decrease in mass (Fig. 2B).

3.2. Cell infiltration in scaffolds pre-treated with collagenase

After observing that collagenase treatment creates specific fiber breakages in TRI scaffolds, thereby opening larger pores, we tested to see if this would facilitate cellular infiltration. MSCs that stably express GFP were seeded on top of TRI scaffolds that had been pre-treated with collagenase solution and then placed into Scaffdex CellCrown™ well inserts (to ensure the scaffold orientation was maintained). MSCs seeded onto the scaffolds were cultured in standard growth media. After two weeks of culture, the samples were fixed and scaffolds sectioned vertically to monitor migration of cells into the scaffold. As can be seen in Fig. 3, panel b, the MSCs remained on the surface of the scaffolds, with negligible cellular infiltration observed.

Given the minimal level of cellular infiltration observed, we questioned whether or not the basal migration level of the GFP-MSCs was too low to observe infiltration into the scaffolds. To stimulate MSC migration, we coated the bottom side of the scaffolds with the chemoattractant platelet derived growth factor (PDGF-BB), which has been shown to be a potent inducer of MSC migration [37-39]. By coating the underside of the scaffold with PDGF-BB, a chemoattractive gradient was created through the scaffold for the MSCs. Despite the pretreatment of scaffolds with collagenase to increase pore sizes in addition to the inclusion of PDGF, there was still negligible cell infiltration at time points of two (Fig. 3, panel c) and three weeks (not shown). Therefore it was apparent that this technique was not an adequate solution for facilitating robust cellular infiltration.

3.3. Reducing the packing density of electrospun fibers

We next developed a modified electrospinning protocol aimed at decreasing the packing density of scaffold fibers. Specifically, a plastic petri dish was used to cover the normal aluminum collecting plate, and twenty evenly spaced holes were created in the petri dish, followed by the placement of 19 gauge needles through the holes touching the grounded collecting plate. A schematic of the collecting plate can be seen in Fig. 4A. During electrospinning, the fibers were attracted to the grounded needles protruding from the petri dish, and bridged from one needle tip to the other. The limited amount of grounded points for fiber attachment reduced the packing density of the electrospun fibers, creating a more three-dimensional scaffold with larger pore sizes. However, it was discovered that this three-

dimensional scaffold fabrication technique was only successful with 100% PCL scaffolds, and could not be replicated with TRI scaffolds (Fig. 4B). SEM confirmed that while the PCL scaffolds showed large pore distribution and channels, the TRI fibers remained densely packed (Fig. 4C). Despite numerous modifications to the protocol, including changes to the solution composition and electrospinning conditions, as well as alterations in the collecting plate set-up, we failed to generate TRI scaffolds with the type of 3-dimensional architecture that was achievable with scaffolds composed of PCL alone. Given the importance of collagen I and nanoHA in stimulating MSC responses critical for osteogenesis, it seems unlikely that the greater porosity of PCL scaffolds spun with multiple grounded needles can compensate for the favorable biochemical signals provided by TRI scaffolds. Hence, alternative electrospinning methods were pursued.

3.4. Inclusion of sacrificial PEO fibers in scaffolds

As another method to increase the pore sizes of TRI scaffolds, the inclusion of sacrificial fibers of the water-soluble polymer poly-(ethylene oxide) was evaluated. By simultaneously electrospinning separate solutions of PEO and TRI, a mixed scaffold was created. After fabrication, soaking the scaffolds in water washed away the sacrificial fibers, leaving just the TRI scaffold with voids where the PEO fibers had previously been. To facilitate the mixing of the fibers onto a flat collecting plate, a fixed gear motor was installed to rotate the collecting plate on an axis parallel to the electrospinning direction. By adding fluorescent dyes to the electrospinning solutions prior to electrospinning, fluorescent microscopy confirmed scaffolds were created with a mixture of two separate fibers, and that the fibers of PEO were removed after soaking in water, leaving just the TRI fibers (Fig. 5A). Furthermore, the removal of PEO was confirmed by comparing the dry weight of the scaffolds before and after soaking them in water (Fig. 5B).

3.5. Measuring the pore sizes of electrospun scaffolds

To quantify the pore sizes of electrospun scaffolds created with sacrificial fibers of PEO, fluorescent confocal microscopy experiments were performed. Electrospun scaffolds of TRI or TRI/PEO were collected onto glass coverslips taped onto the rotating collecting plate. To ensure equal fiber distribution, equal volumes of TRI solution were electrospun. TRI solutions were stained with fluorescent dye ($DiOC_{18}(3)$) prior to electrospinning. After soaking in water, scaffolds were imaged using a Zeiss confocal microscope. Individual scans of the samples were combined to create a 10 μm thick picture. NIS-Elements software was used to analyze the resulting images. 25 pores were selected at random using the Area Auto Detect feature. In Fig. 6A, representative images are shown to illustrate boundary selection by the software. The mean pore size in TRI scaffolds created with sacrificial fibers of PEO was 1826.11 μm^2, significantly greater than the mean size of pores for TRI scaffolds created without PEO fibers (424 μm^2) (Fig. 6B).

3.6. MSC infiltration in scaffolds with PEO fibers

After successful fabrication of scaffolds consisting of separate TRI and PEO fibers, scaffolds were evaluated for the effect of PEO fiber removal on cellular infiltration. Electrospun scaffolds of TRI/PEO were first soaked in water overnight to remove the PEO fibers. Scaffolds were then loaded into Scaffdex holders to maintain their orientation and seeded with MSCs. TRI scaffolds created without PEO were used as controls. After one week in culture, the samples were fixed and vertical sections of the scaffolds were stained with DAPI to visualize the nuclei of cells infiltrating into the scaffold. As can be seen in Fig. 7A, MSCs were present within the interior of the TRI/PEO scaffolds, showing that removal of sacrificial fibers facilitated cellular infiltration. In comparison, MSCs were only present on the surface of TRI scaffolds created without PEO.

In order to quantify the amount of cellular infiltration observed in these experiments, a custom MATLAB script was created to process the images. Phase contrast and DAPI images were taken of the scaffold cross-sections and loaded into the MATLAB program. The phase contrast image was used in order to set the boundaries of the scaffold and calculate the thickness of the scaffold. The scaffold boundaries were then mapped onto the DAPI image, and the script calculated the distance from each cell nuclei to the top of the scaffold. Results of this analysis showed that TRI scaffolds created with PEO had an average cell infiltration of 45.49 μm, compared to 6.13 μm for TRI scaffolds without PEO (Fig. 7B), confirming that sacrificial fibers of PEO facilitate cellular infiltration of MSCs.

3.7. Infiltration of endogenous cells from calvarial organ cultures

To examine the infiltration of endogenous cells from a bone microenvironment, a mouse organ culture model was used. This *ex-vivo* model has numerous advantages over *in vitro* cell migration assays. The excised calvariae retain the three-dimensional architecture of developing bones and also possess the relevant cell types found in bone, including osteoblasts, osteocytes, stromal and pre-osteoblastic cells [36,40]. With all of these different cell types interacting with one another through paracrine and endocrine signaling molecules, this model provides a physiologically-relevant environment to study cellular infiltration of bone cells. Excised calvariae from neonatal mice were placed into culture on top of a steel grid to keep them from floating and hold them at the liquid/air interface. TRI or TRI/PEO (previously soaked in water to remove PEO) scaffolds were placed directly on top of the calvariae, where they come into contact with the bone-lining cells. After 8 days in culture, the calvaria/scaffold constructs were fixed and vertical sections were stained with DAPI to show cellular nuclei. As can be seen in Fig. 8A, TRI scaffolds created with sacrificial fibers of PEO showed greater cellular infiltration of cells from the mouse calvaria into the scaffold.

In order to quantify the distance traveled by infiltrating endogenous cells, a custom MATLAB script was used as outlined above. Results of this analysis showed that cells on TRI/PEO scaffolds were able to infiltrate 63.15 μm on average, compared to 20.06 μm for cells on regular TRI scaffolds (Fig. 8B). Collectively these results confirm that sacrificial fibers of PEO can be included in the electrospinning process in order to create electrospun scaffolds that facilitate the infiltration of MSCs and endogenous bone cells.

4. Discussion

As the average age of the current population continues to increase, the need for bone grafts to repair skeletal defects will correspondingly rise [6]. Therefore, creating a synthetic bone graft that can replace or supplement autografted bone has become a major goal in the field of tissue engineering [7,41]. One of the more promising techniques for fabricating a synthetic bone graft is the process of electrospinning, due to the ease in creating a nanofibrous matrix that mimics natural ECM structure [42,43]. Additionally, by combining synthetic and biological components, more complex, bone-mimetic scaffolds can be created that have tunable mechanical and resorbable properties (enabled by the synthetic polymer) while providing important biologic cues (from bone-derived molecules) to osteogenic cells [44]. As an example, several investigators have studied the incorporation of collagen I and hydroxyapatite into electrospun scaffolds since these two molecules comprise the principal constituents of bone ECM. These studies have shown that electrospun nanofibers that have incorporated HA [15,16,45] and/or collagen [17-19,46] facilitate the adhesion, proliferation, and osteoblastic differentiation of bone cells *in vitro* as well as support robust bone formation *in vivo*.

Although these results show promise toward the end goal of creating a synthetic bone graft, there is a significant limitation associated with electrospun scaffolds. Due to the dense

packing of electrospun nanofibers during the fabrication process, the resulting matrix has very small pore sizes, which hinders the infiltration of cells *in vitro* and limits tissue-ingrowth and vascularization *in vivo* [20,21,47]. In order to maximize the success of a biodegradable implant, the implant must support the infiltration of bone cells throughout the thickness of the material, allowing the implant to be replaced with native bone over time through the process of creeping substitution [48]. Additionally, vascularization of the biomaterial is an essential step in tissue healing, as this process provides the nutrients and oxygen needed for bone cells to survive, while facilitating removal of waste products from cell metabolism [20,21,47,49]. Accordingly, a growing focus in the field of tissue engineering is to discover techniques that increase the mean pore sizes of electrospun scaffolds and thereby facilitate cellular infiltration.

In this study, we investigated several techniques for creating bone-mimetic TRI scaffolds that have permissive pore sizes for cellular infiltration. We initially observed that limited treatment of the bone-mimetic scaffolds with a collagenase solution *in vitro* created specific fiber breakages throughout the scaffold, thereby opening up larger pores. However, it was observed that the pores created by collagenase treatment were insufficient to allow MSC infiltration. As a second approach, we developed a modified electrospinning protocol with the goal of decreasing fiber packing density, creating larger pores between the fibers. Several groups have similarly attempted to decrease fiber packing density using a variety of methods. Mitchell and Sanders reported the creation of a controlled electrospinning set-up in order to tightly control fiber diameter and inter-fiber spacing [50]. Although cell infiltration was not evaluated, it was found that the dielectric strength of the collecting plate had a significant effect on inter-fiber spacing. Vaquette and Cooper–White tested a number of patterned collecting plates, and determined that electrospun PCL fibers would collect along the patterns of the plate [51]. Some of these patterns could be used to create larger pores, and the resulting scaffolds facilitated infiltration of NIH 3T3 fibroblasts. Soliman et al. tested both micro- and nanofiber meshes of either low or high density fiber packing and found that the microfiber low density fiber packing scaffolds supported the greatest cell infiltration of GFP-HUVECs [21]. Lastly, Blakeney et al. were able to significantly decrease the packing density of electrospun PCL scaffolds by using a custom collecting surface consisting of a spherical foam bowl with an array of embedded stainless steel probes [29]. The resulting electrospun scaffold possessed a fluffy, three-dimensional structure, which supported high levels of INS-1 cell infiltration *in vitro*. These collective results from multiple investigators provide excellent support for the concept of increasing pore size through controlled fiber packing, however it should be noted that all of these prior studies were performed with single polymer solutions (e.g. 100% PCL). In the current study, we created a unique collecting plate consisting of 19 gauge needles protruding perpendicularly through a plastic petri dish. This strategy was very successful for scaffolds composed of 100% PCL; the scaffolds formed in biscuit- like sheets, with very loosely packed fibers between the sheets. Additionally, the scaffolds had a wide range of pore sizes and deep channels, creating a structure resembling natural trabecular bone. Unfortunately, these results could not be replicated using our bone-mimetic scaffolds, despite many adaptations to the protocol including changing the needle gauge, needle density, electrospinning voltage, solution viscosity, and the replacement of the plastic collecting plate with Styrofoam. Clearly there is a need for further studies aimed at adapting novel electrospinning protocols for use with complex scaffolds incorporating biologic molecules. In this regard, Hutmacher's group used a combination of electrospinning and electrospraying to create PCL/col electrospun scaffolds with pockets of hyaluronan gel; this approach was very effective in promoting infiltration of multiple cell types [22,47].

Another emerging method for increasing scaffold porosity involves the incorporation of sacrificial fibers of PEO during the electrospinning process. This technique was first

reported by Baker et al. [31], and its effectiveness has since been confirmed by others [24,32]. However, to our knowledge, PEO fibers have yet to be utilized in conjunction with bone-mimetic fibers mixing collagen I, nanoHA and PCL, creating a complex, tissue-specific matrix. In the current study, composite fibers of PCL/col/HA were co-spun with separate fibers of PEO. Washing the scaffolds removed the PEO fibers, leaving larger voids in the matrix between the remaining PCL/col/HA fibers. Increased pore size was confirmed by fluorescent confocal microscope and NIS-Elements imaging software. In order to evaluate the effectiveness of using sacrificial fibers to promote cellular infiltration, MSCs were grown on the TRI scaffolds created with PEO fibers and the positions of nuclei on scaffold cross-sections were measured. It was observed that scaffolds created with PEO fibers were able to support a significantly greater level of cellular infiltration compared to scaffolds created without PEO fibers. These data establish that the inclusion of sacrificial fibers of PEO can be readily adapted to more complex electrospun scaffolds consisting of composite fibers designed to mimic a specific natural extracellular matrix. In future studies one important objective will be to test varying amounts of PEO in bone-mimetic scaffolds, with the goal of tailoring PEO fiber number to control the degree of cell infiltration. Previous studies by others [31,32] have shown a positive correlation between the degree of cell infiltration and the percentage of PEO within electrospun PCL scaffolds.

Although *in vitro* studies of cell infiltration are commonly employed to evaluate the effects of scaffold pore size, few investigators have monitored scaffold infiltration by endogenous cells within bone matrix. Due to the complexity of intact tissues, where numerous cell types and soluble factors cooperate to regulate cell and tissue responses, it can be difficult to accurately model bone cell behavior. Therefore we felt it was essential to examine cell infiltration in a more physiologically-relevant system. This was accomplished by using a mouse calvarial organ culture. In this *ex vivo* model, the calvaria retain the three-dimensional architecture of developing bones and also possess the relevant cell types found in bone, which constantly interact with one another in a bone microenvironment [36,40]. Our results show that cells from the natural bone matrix interact favorably with the PCL/col/HA scaffolds; specifically, cells were able to migrate from the calvaria and attach to the surface of the these scaffolds. Most importantly, significantly greater cell infiltration was observed in TRI matrices created with PEO fibers. These results provide strong evidence that matrices composed of PCL/col/HA are not only effective in promoting bone cell adhesion and survival, but the further inclusion of sacrificial PEO fibers represents a successful and technically straightforward method for enhancing porosity, leading to enhanced cell infiltration.

5. Conclusion

In prior studies electrospun PCL/col/HA scaffolds were developed that supported greater MSC adhesion, signaling and proliferation as compared with scaffolds composed of PCL or collagen I alone, however the small pore sizes of these bone-mimetic scaffolds limited cell infiltration. In this investigation, we evaluated the efficacy of multiple techniques in increasing the pore size of the PCL/col/HA scaffolds, thereby enhancing cell infiltration. We found that incorporation of PEO sacrificial fibers in the electrospinning process facilitated MSC infiltration *in vitro*, as well as infiltration of endogenous cells when scaffolds were placed within calvarial organ cultures. While there is currently much interest in developing methods to increase the pore size of electrospun scaffolds, few of these have been adapted for use with multi-component scaffolds incorporating biologic molecules. Results from this study show that electrospinning PEO sacrificial fibers is a relatively simple approach that can be used with complex tissue-mimicking electrospun scaffolds to increase cell infiltration. More importantly, the enhanced cell infiltration achieved by incorporating PEO

sacrificial fibers overcomes one of the major limitations of bone-mimetic PCL/col/HA matrices, which have already shown promise as supportive matrices for osteoregeneration.

Acknowledgments

This research was supported by NIH/NIAMS grant R01AR51539 (SLB) and MC Phipps is supported by the NIH Nanotechnology in Biosensors and Bioengineering grant 5T32EB004312-04 (Vohra, YK). The authors gratefully acknowledge the Bone Histomorphometry Core Facility for their assistance with tissue processing and staining, the High Resolution Imaging Facility for their assistance with confocal microscope imaging, the Central Analytical Facility (University of Alabama) and Robin Foley Ph.D. (UAB) for their assistance with SEM imaging. MC Phipps would also like to acknowledge the Howard Hughes Institute Med to Grad Fellowship program.

References

1. Hing KA. Bone repair in the twenty-first century: biology, chemistry or engineering? Philos Transact A Math Phys Eng Sci. 2004; 362:2821–50. [PubMed: 15539372]
2. Brighton CT, Shaman P, Heppenstall RB, Esterhai JL, Pollack SR, Friedenberg ZB. Tibial nonunion treated with direct-current, capacitive coupling, or bone-graft. Clin Orthop Relat Res. 1995:223–34. [PubMed: 7497673]
3. Fernyhough JC, Schimandle JJ, Weigel MC, Edwards CC, Levine AM. Chronic donor site pain complicating bone-graft harvesting from the posterior iliac crest for spinal-fusion. Spine. 1992; 17:1474–80. [PubMed: 1471005]
4. Goulet JA, Senunas LE, DeSilva GL, Greenfield MLVH. Autogenous iliac crest bone graft - complications and functional assessment. Clin Orthop Relat Res. 1997; 339:76–81. [PubMed: 9186204]
5. Giannoudis PV, Dinopoulos H, Tsiridis E. Bone substitutes: an update. Injury. 2005; 36(Suppl 3):S20–7. [PubMed: 16188545]
6. Brydone AS, Meek D, Maclaine S. Bone grafting, orthopaedic biomaterials, and the clinical need for bone engineering. Proc Inst Mech Eng H. 2010; 224:1329–43. [PubMed: 21287823]
7. Navarro M, Michiardi A, Castano O, Planell JA. Biomaterials in orthopaedics. J R Soc Interface. 2008; 5:1137–58. [PubMed: 18667387]
8. Huang ZM, Zhang YZ, Kotaki M, Ramakrishna S. A review on polymer nanofibers by electrospinning and their applications in nanocomposites. Compos Sci Technol. 2003; 63:2223–53.
9. Pham QP, Sharma U, Mikos AG. Electrospinning of polymeric nanofibers for tissue engineering applications: a review. Tissue Eng. 2006; 12:1197–211. [PubMed: 16771634]
10. Murugan R, Ramakrishna S. Nano-featured scaffolds for tissue engineering: a review of spinning methodologies. Tissue Eng. 2006; 12:435–47. [PubMed: 16579677]
11. Prabhakaran MP, Venugopal J, Ramakrishna S. Electrospun nanostructured scaffolds for bone tissue engineering. Acta Biomater. 2009; 5:2884–93. [PubMed: 19447211]
12. Venugopal J, Low S, Choon AT, Kumar TSS, Ramakrishna S. Mineralization of osteoblasts with electrospun collagen/hydroxyapatite nanofibers. J Mater Sci Mater Med. 2008; 19:2039–46. [PubMed: 17957448]
13. Wutticharoenmongkol P, Sanchavanakit N, Pavasant P, Supaphol P. Preparation and characterization of novel bone scaffolds based on electrospun polycaprolactone fibers filled with nanoparticles. Macromol Biosci. 2006; 6:70–7. [PubMed: 16374772]
14. Catledge SA, Clem WC, Shrikishen N, Chowdhury S, Stanishevsky AV, Koopman M, et al. An electrospun triphasic nanofibrous scaffold for bone tissue engineering. Biomed Mater. 2007; 2:142–50. [PubMed: 18458448]
15. Gupta D, Venugopal J, Mitra S, Giri Dev VR, Ramakrishna S. Nanostructured biocomposite substrates by electrospinning and electrospraying for the mineralization of osteoblasts. Biomaterials. 2009; 30:2085–94. [PubMed: 19167752]
16. Lao L, Wang Y, Zhu Y, Zhang Y, Gao C. Poly(lactide-co-glycolide)/hydroxyapatite nanofibrous scaffolds fabricated by electrospinning for bone tissue engineering. J Mater Sci Mater Med. 2011; 22:1873–84. [PubMed: 21681656]

17. Ekaputra AK, Zhou Y, Cool SM, Hutmacher DW. Composite electrospun scaffolds for engineering tubular bone grafts. Tissue Eng Part A. 2009; 15:3779–88. [PubMed: 19527183]
18. Chan CK, Liao S, Li B, Lareu RR, Larrick JW, Ramakrishna S, et al. Early adhesive behavior of bone-marrow-derived mesenchymal stem cells on collagen electrospun fibers. Biomed Mater. 2009; 4:035006. [PubMed: 19439824]
19. Phipps MC, Clem WC, Catledge SA, Xu Y, Hennessy KM, Thomas V, et al. Mesenchymal stem cell responses to bone-mimetic electrospun matrices composed of polycaprolactone, collagen I and nanoparticulate hydroxyapatite. PLoS One. 2011; 6:e16813. [PubMed: 21346817]
20. Karageorgiou V, Kaplan D. Porosity of 3D biomaterial scaffolds and osteogenesis. Biomaterials. 2005; 26:5474–91. [PubMed: 15860204]
21. Soliman S, Sant S, Nichol JW, Khabiry M, Traversa E, Khademhosseini A. Controlling the porosity of fibrous scaffolds by modulating the fiber diameter and packing density. J Biomed Mater Res A. 2011; 96:566–74. [PubMed: 21254388]
22. Ekaputra AK, Prestwich GD, Cool SM, Hutmacher DW. Combining electrospun scaffolds with electrosprayed hydrogels leads to three-dimensional cellularization of hybrid constructs. Biomacromolecules. 2008; 9:2097–103. [PubMed: 18646822]
23. Nerurkar NL, Sen S, Baker BM, Elliott DM, Mauck RL. Dynamic culture enhances stem cell infiltration and modulates extracellular matrix production on aligned electrospun nanofibrous scaffolds. Acta Biomater. 2011; 7:485–91. [PubMed: 20728589]
24. Milleret V, Simona B, Neuenschwander P, Hall H. Tuning electrospinning parameters for production of 3D-fiber-fleeces with increased porosity for soft tissue engineering applications. Eur Cell Mater. 2011; 21:286–303. [PubMed: 21432783]
25. Pham QP, Sharma U, Mikos AG. Electrospun poly(epsilon-caprolactone) microfiber and multilayer nanofiber/microfiber scaffolds: characterization of scaffolds and measurement of cellular infiltration. Biomacromolecules. 2006; 7:2796–805. [PubMed: 17025355]
26. Nam J, Huang Y, Agarwal S, Lannutti J. Improved cellular infiltration in electrospun fiber via engineered porosity. Tissue Eng. 2007; 13:2249–57. [PubMed: 17536926]
27. Wright LD, Andric T, Freeman JW. Utilizing NaCl to increase the porosity of electrospun materials. Mater Sci Eng C Mater Biol Appl. 2010; 31:30–6.
28. Leong MF, Rasheed MZ, Lim TC, Chian KS. In vitro cell infiltration and in vivo cell infiltration and vascularization in a fibrous, highly porous poly(D, L-lactide) scaffold fabricated by cryogenic electrospinning technique. J Biomed Mater Res A. 2009; 91:231–40. [PubMed: 18814222]
29. Blakeney BA, Tambralli A, Anderson JM, Andukuri A, Lim DJ, Dean DR, et al. Cell infiltration and growth in a low density, uncompressed three-dimensional electrospun nanofibrous scaffold. Biomaterials. 2011; 32:1583–90. [PubMed: 21112625]
30. Lee JB, Jeong SI, Bae MS, Yang DH, Heo DN, Kim CH, et al. Highly porous electrospun nanofibers enhanced by ultrasonication for improved cellular infiltration. Tissue Eng Part A. 2011 E-pub ahead of print.
31. Baker BM, Gee AO, Metter RB, Nathan AS, Marklein RA, Burdick JA, et al. The potential to improve cell infiltration in composite fiber-aligned electrospun scaffolds by the selective removal of sacrificial fibers. Biomaterials. 2008; 29:2348–58. [PubMed: 18313138]
32. Whited BM, Whitney JR, Hofmann MC, Xu Y, Rylander MN. Pre-osteoblast infiltration and differentiation in highly porous apatite-coated PLLA electrospun scaffolds. Biomaterials. 2011; 32:2294–304. [PubMed: 21195474]
33. Hennessy KM, Clem WC, Phipps MC, Sawyer AA, Shaikh FM, Bellis SL. The effect of RGD peptides on osseointegration of hydroxyapatite biomaterials. Biomaterials. 2008; 29:3075–83. [PubMed: 18440064]
34. Culpepper BK, Phipps MC, Bonvallet PP, Bellis SL. Enhancement of peptide coupling to hydroxyapatite and implant osseointegration through collagen mimetic peptide modified with a polyglutamate domain. Biomaterials. 2010; 31:9586–94. [PubMed: 21035181]
35. Kilpadi KL, Sawyer AA, Prince CW, Chang PL, Bellis SL. Primary human marrow stromal cells and Saos-2 osteosarcoma cells use different mechanisms to adhere to hydroxylapatite. J Biomed Mater Res. 2004; 68A:273–85.

36. Mohammad KS, Chirgwin JM, Guise TA. Assessing new bone formation in neonatal calvarial organ cultures. Methods Mol Biol. 2008; 455:37–50. [PubMed: 18463809]
37. Ozaki Y, Nishimura M, Sekiya K, Suehiro F, Kanawa M, Nikawa H, et al. Comprehensive analysis of chemotactic factors for bone marrow mesenchymal stem cells. Stem Cells Dev. 2007; 16:119–29. [PubMed: 17348810]
38. Allori AC, Sailon AM, Warren SM. Biological basis of bone formation, remodeling, and repair-part I: biochemical signaling molecules. Tissue Eng Part B Rev. 2008; 14:259–73. [PubMed: 18665803]
39. Alvarez RH, Kantarjian HM, Cortes JE. Biology of platelet-derived growth factor and its involvement in disease. Mayo Clin Proc. 2006; 81:1241–57. [PubMed: 16970222]
40. Garrett IR. Assessing bone formation using mouse calvarial organ cultures. Methods Mol Med. 2003; 80:183–98. [PubMed: 12728719]
41. Frohlich M, Grayson WL, Wan LQ, Marolt D, Drobnic M, Vunjak-Novakovic G. Tissue engineered bone grafts: biological requirements, tissue culture and clinical relevance. Curr Stem Cell Res Ther. 2008; 3:254–64. [PubMed: 19075755]
42. Ifkovits JL, Sundararaghavan HG, Burdick JA. Electrospinning fibrous polymer scaffolds for tissue engineering and cell culture. J Vis Exp. 2009; 3210.3791/1589
43. Li WJ, Tuan RS. Fabrication and application of nanofibrous scaffolds in tissue engineering. Curr Protoc Cell Biol. 2009; Chap. 25(Unit 25):2. [PubMed: 19283731]
44. Nisbet DR, Forsythe JS, Shen W, Finkelstein DI, Horne MK. Review paper: a review of the cellular response on electrospun nanofibers for tissue engineering. J Biomater Appl. 2009; 24:7–29. [PubMed: 19074469]
45. Fu YC, Nie H, Ho ML, Wang CK, Wang CH. Optimized bone regeneration based on sustained release from three-dimensional fibrous PLGA/HAp composite scaffolds loaded with BMP-2. Biotechnol Bioeng. 2008; 99:996–1006. [PubMed: 17879301]
46. Lee JJ, Yu HS, Hong SJ, Jeong I, Jang JH, Kim HW. Nanofibrous membrane of collagen-polycaprolactone for cell growth and tissue regeneration. J Mater Sci Mater Med. 2009; 20:1927–35. [PubMed: 19365614]
47. Ekaputra AK, Prestwich GD, Cool SM, Hutmacher DW. The three-dimensional vascularization of growth factor-releasing hybrid scaffold of poly (varepsilon-caprolactone)/collagen fibers and hyaluronic acid hydrogel. Biomaterials. 2011; 32:8108–17. [PubMed: 21807407]
48. Nuss KM, von Rechenberg B. Biocompatibility issues with modern implants in bone - a review for clinical orthopedics. Open Orthop J. 2008; 2:66–78. [PubMed: 19506701]
49. Jain RK, Au P, Tam J, Duda DG, Fukumura D. Engineering vascularized tissue. Nat Biotechnol. 2005; 23:821–3. [PubMed: 16003365]
50. Mitchell SB, Sanders JE. A unique device for controlled electrospinning. J Biomed Mater Res A. 2006; 78:110–20. [PubMed: 16604530]
51. Vaquette C, Cooper-White JJ. Increasing electrospun scaffold pore size with tailored collectors for improved cell penetration. Acta Biomater. 2011; 7:2544–57. [PubMed: 21371575]

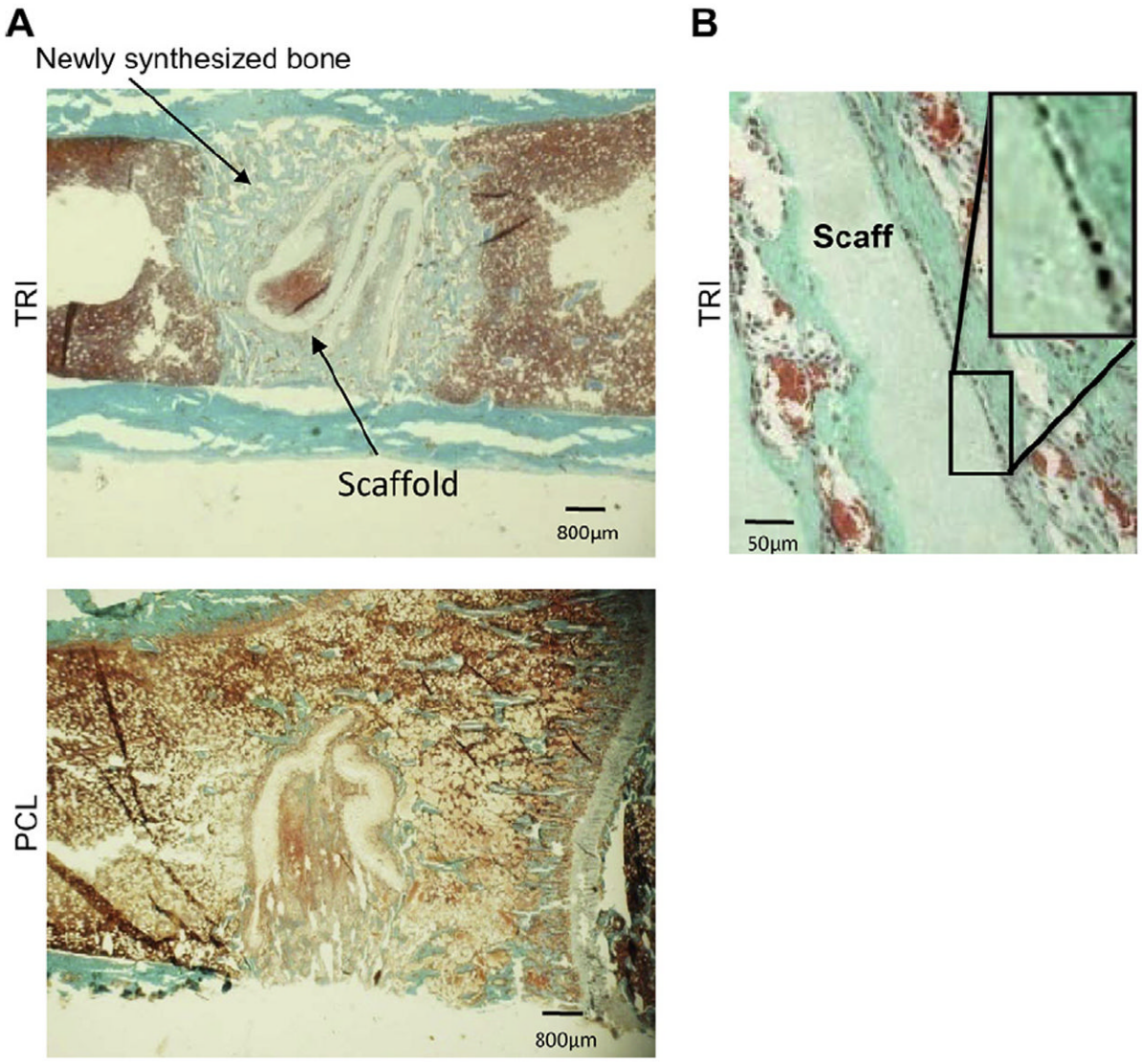

Fig. 1.

PCL/col/HA scaffolds (“TRI”), or scaffolds composed of 100% PCL, were implanted into a cortical defect in a rat tibia for seven days. A) Low magnification images of transverse sections stained with Goldner’s Trichrome show new bone stained light blue-green, soft tissue stained red, and cell nuclei stained black. TRI scaffolds supported robust new bone formation throughout the defect (A), especially in direct contact with the scaffold surface (B). However, endogenous cells can be seen lining the edge of scaffolds (B inset). The small pore sizes of electrospun TRI scaffolds hinder cell infiltration and tissue-ingrowth. (For interpretation of the references to colour in this figure legend, the reader is referred to the web version of this article.)

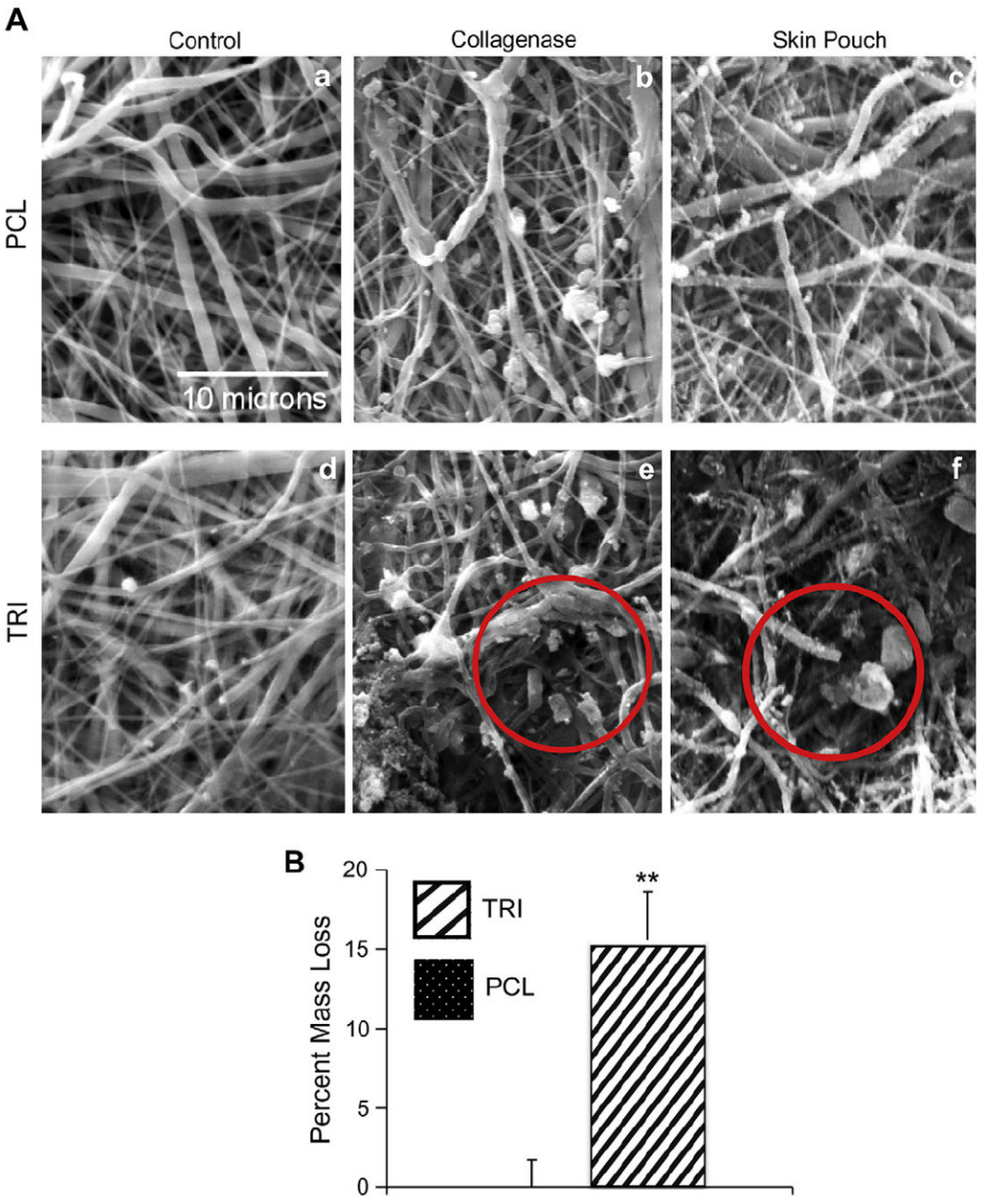

Fig. 2.

SEM images of selective cleavage of collagen I present in TRI scaffolds. A) Treatment with collagenase solution *in vitro* (b, e) or exposure to endogenous collagenases in a rat subcutaneous skin pouch (c, f) are able to cleave the collagen within fibers of TRI scaffolds creating larger pores (red circles), but have no effect on PCL scaffolds. B) Weighing the scaffolds before and after soaking in collagenase solution verified cleavage of collagen fibers in TRI scaffolds. An ** denotes $p < .001$. (For interpretation of the references to colour in this figure legend, the reader is referred to the web version of this article.)

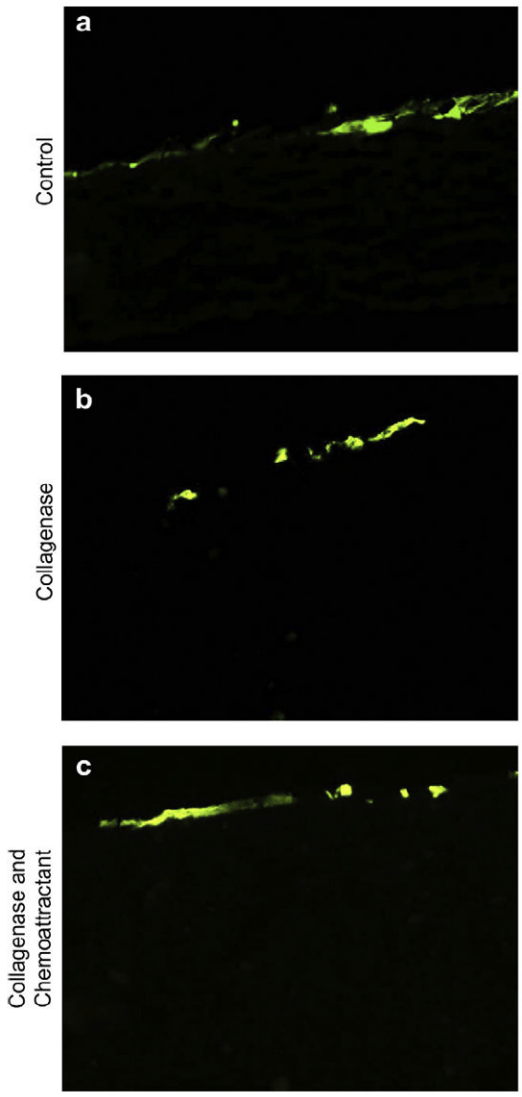

Fig. 3.

Pre-treating scaffolds with collagenase does not facilitate cell infiltration of MSCs *in vitro*. GFP-expressing MSCs were seeded onto TRI scaffolds previously treated with collagenase to create larger pores, or untreated scaffolds as a control. After two weeks, samples were fixed and sectioned to evaluate MSC infiltration into the scaffolds (a and b). Collagenase treatment did not facilitate significant cellular infiltration. In attempt to stimulate cellular infiltration, PDGF-BB, a known MSC chemoattractant, was added to the underside of scaffolds after collagenase treatment and prior to cell seeding. This was done to create a chemoattractive gradient through the scaffold. MSC infiltration remained minimal (c).

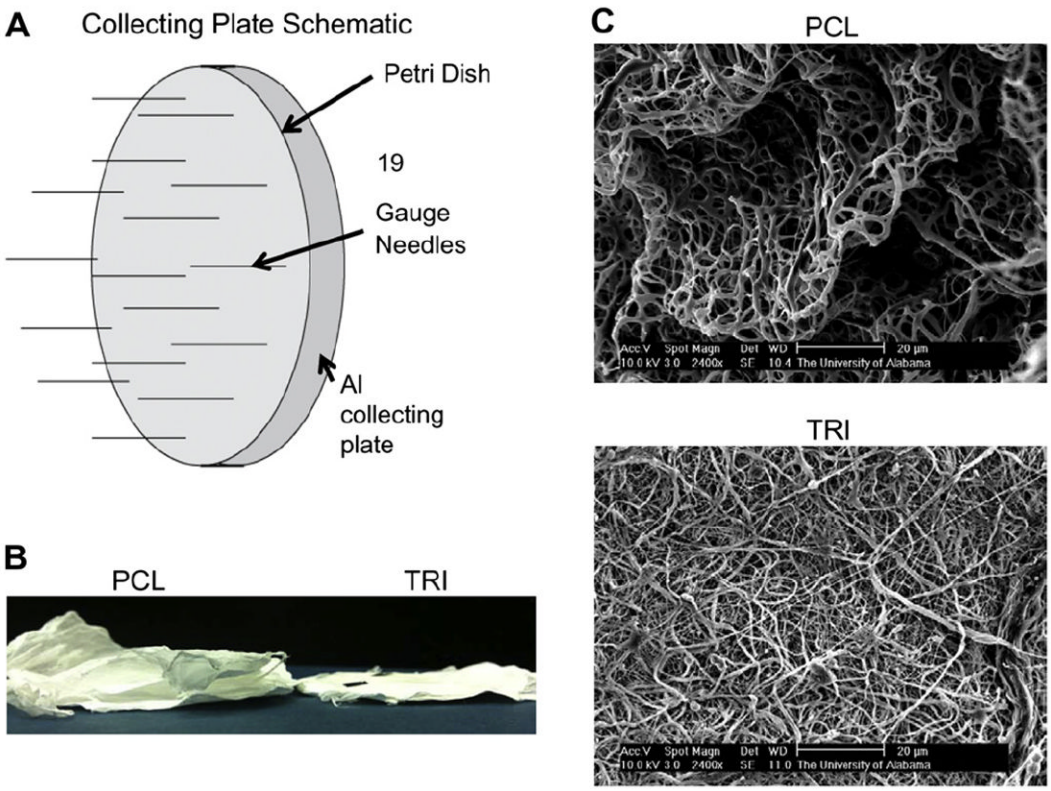

Fig. 4.

Decreasing the packing density of electrospun fibers. A unique collecting plate was used in order to decrease the packing density of electrospun fibers and therefore create larger pores (A). Although 100% PCL scaffolds formed in loosely packed layers (B) and possessed a favorable 3-dimensional architecture with deep channels (C), these results were not observed when TRI scaffolds were electrospun using the same collecting plate.

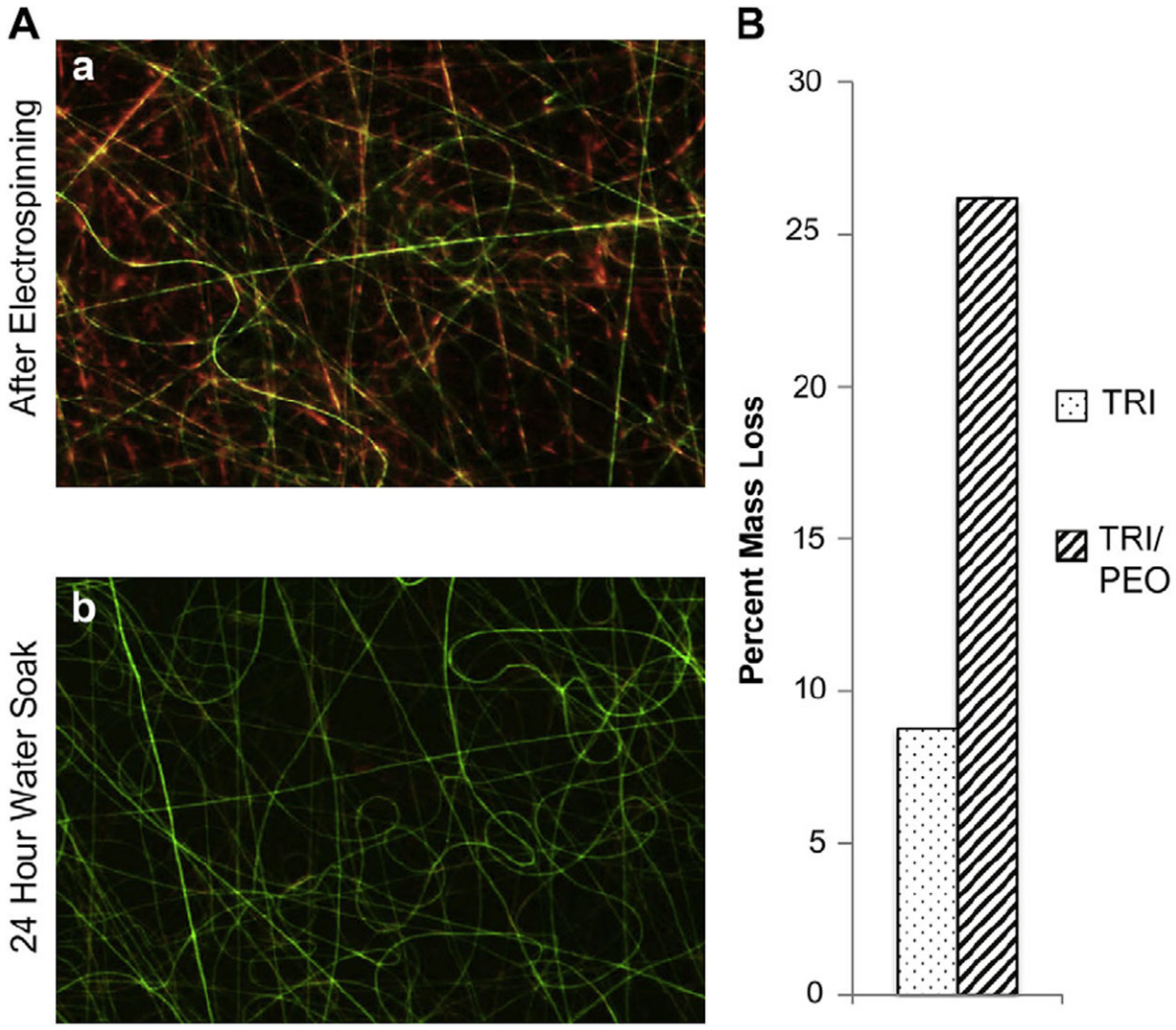

Fig. 5.

Removal of sacrificial electrospun fibers. A) As an alternative method to increase pore sizes, water-soluble fibers of PEO were incorporated into TRI scaffolds. Fluorescent dyes confirmed that separate fibers of PEO (Red) and TRI (Green) were intermixed in the scaffold (a). After washing scaffolds in water, PEO fibers were removed (b). B) Weighing the scaffolds before and after washing indicated removal of PEO fibers by mass loss. (For interpretation of the references to colour in this figure legend, the reader is referred to the web version of this article.)

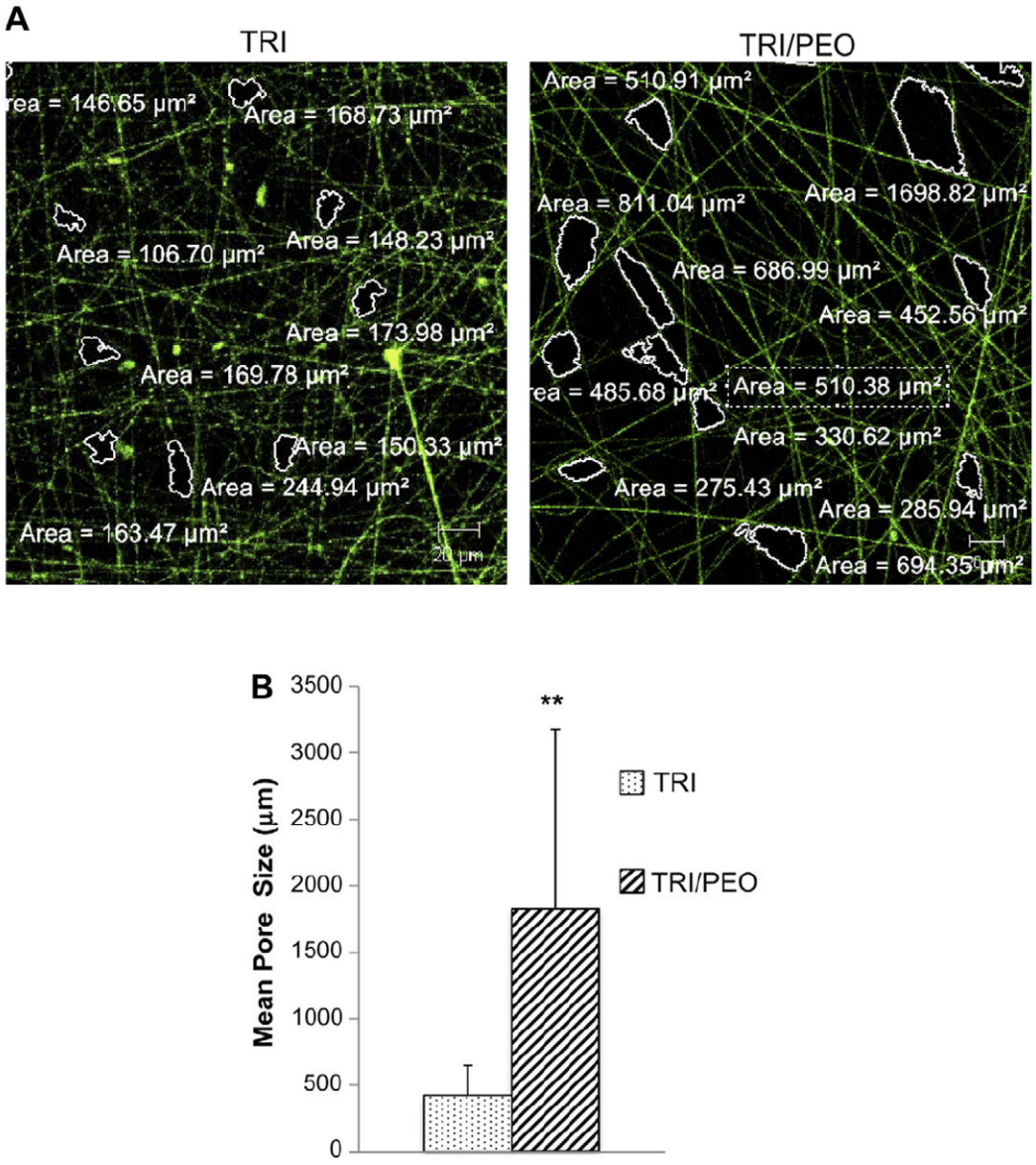

Fig. 6.

Mean pore size analysis of electrospun TRI and TRI/PEO scaffolds. A) Fluorescently stained TRI/PEO scaffolds (washed to remove PEO) or TRI scaffolds electrospun without PEO fibers were visualized using a Zeiss confocal microscope. The area of 25 pores manually selected at random were measured using the auto area detect feature of NIS-Elements software. B) The mean pore size of TRI/PEO scaffolds was significantly greater than TRI scaffolds. An ** denotes $p < .0001$.

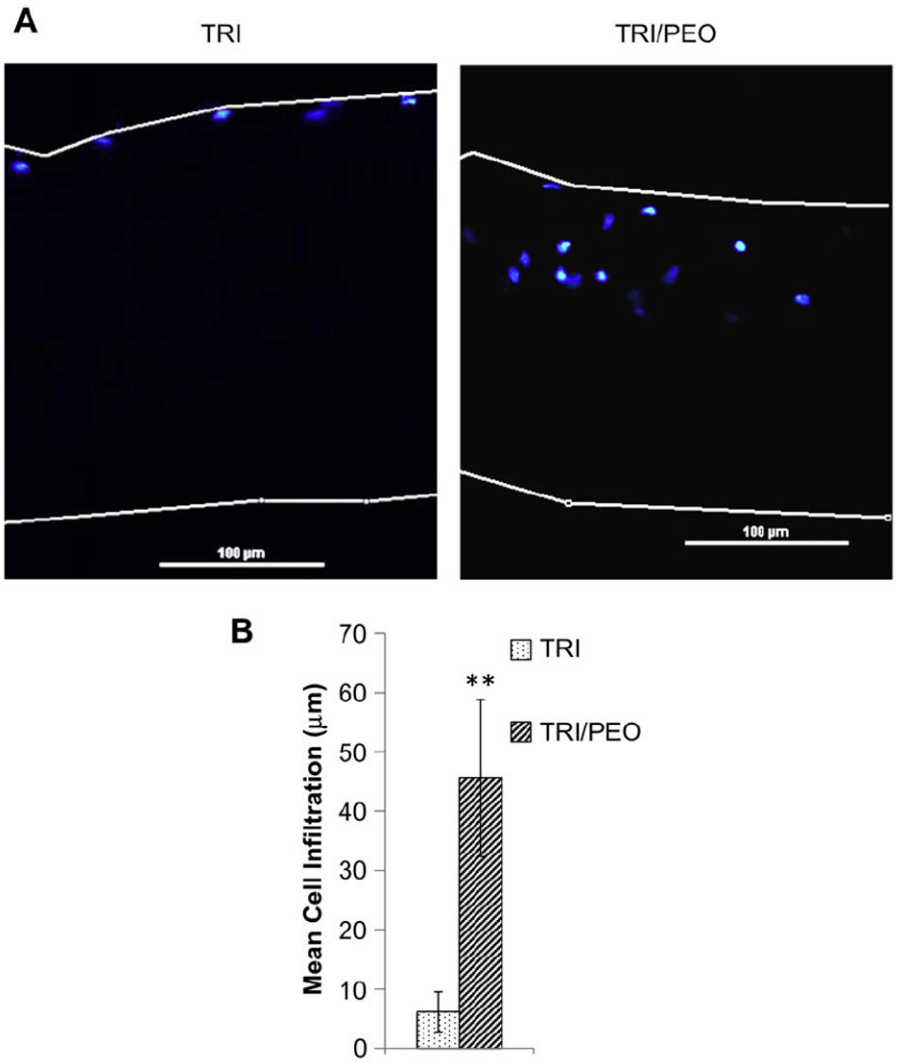

Fig. 7.

Electrospun scaffolds created with PEO fibers support cell infiltration of MSCs *in vitro*. After removal of PEO fibers from TRI/PEO scaffolds by washing, MSCs were seeded for one week. A) Scaffolds were sectioned and stained with DAPI to show cellular nuclei location. MSCs were able to infiltrate into the TRI/PEO scaffolds, but not TRI scaffolds, as seen by presence of nuclei within TRI/PEO scaffolds. B) Cell infiltration was quantified using a custom MatLab script. On average, MSCs seeded on TRI/PEO scaffolds migrated 45.59 μm into the scaffold, significantly greater than infiltration on TRI scaffolds (6.13 μm). An ** denotes $p < .0001$.

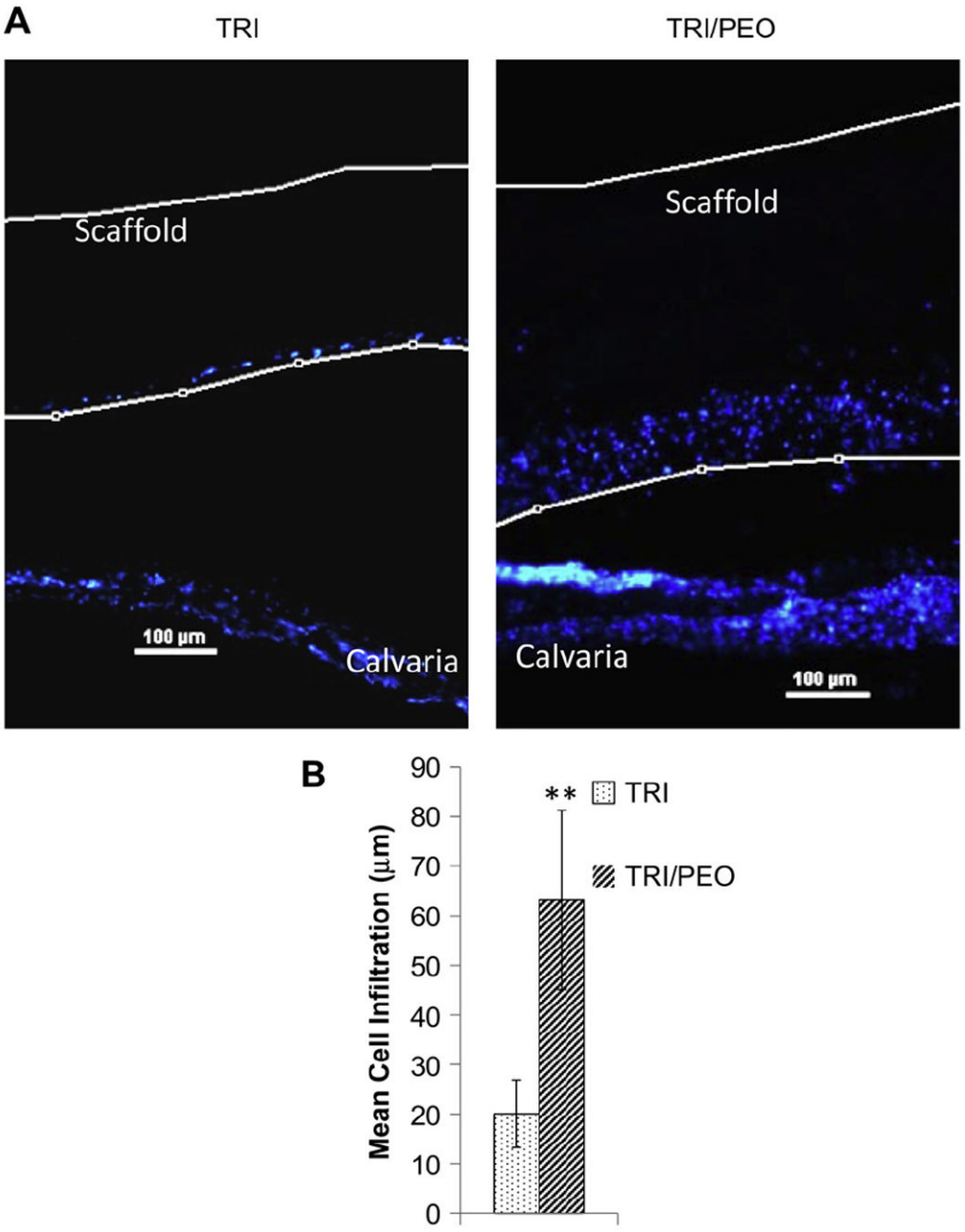

Fig. 8.

Electrospun scaffolds created with PEO fibers support infiltration of endogenous cells from calvarial organ cultures. After removal of PEO fibers from TRI/PEO scaffolds by washing, scaffolds were placed directly on top of excised calvaria from neonatal mice. After 8 days in culture, the scaffold/calvaria constructs were fixed and vertical sections were stained with DAPI to show cellular nuclei location (it should be noted that the apparent gap between the scaffold and the calvaria is an artifact introducing during processing and sectioning of the samples). A) Endogenous cells were observed within the TRI/PEO scaffolds, while remaining largely on the surface of TRI scaffolds. B) Cell infiltration was quantified using a custom MatLab script. On average, endogenous bone cells migrated 63.15 μm into TRI/

PEO scaffolds, which was significantly greater than infiltration levels observed on TRI scaffolds (20.06 μm). An ** denotes $p < .0001$